Journal of Chromatography, 395 (1987) 91–110
Elsevier Science Publishers B.V., Amsterdam — Printed in The Netherlands

CHROMSYMP. 1089

CALCULATION OF PRESSURE, DENSITY AND TEMPERATURE PROFILES IN PACKED-COLUMN SUPERCRITICAL FLUID CHROMATOGRAPHY

PETER J. SCHOENMAKERS*
Philips Research Laboratories, P.O. Box 80 000, 5600 JA Eindhoven (The Netherlands)
PAUL E. ROTHFUSZ
Philips Centre for Manufacturing Technology (CFT), 5600 MD Eindhoven (The Netherlands)
and
FRANK C. C. J. G. VERHOEVEN
Philips Research Laboratories, P.O. Box 80 000, 5600 JA Eindhoven (The Netherlands)

SUMMARY

The simultaneous calculation of pressure, density and temperature profiles for packed columns used in supercritical fluid chromatography (SFC) is described. The profiles are obtained by solving the heat balance equation numerically at a large number of locations in the column. The compressibility of the mobile phase (carbon dioxide) and the variations of the isochoric heat capacity, thermal conductivity and viscosity with temperature and pressure are taken into account.

The results show that pressure profiles over packed columns in SFC are approximately linear. At high mobile phase densities, a supercritical fluid behaves like a liquid, but the viscosity is much lower. The temperature increases slightly along the column length. At lower densities the compressibility of the fluid becomes more apparent. The density decreases along the column length and so does the temperature of the eluent. Both the variations in density and in temperature are enhanced by using smaller particles or higher flow-rates. Temperature effects are reduced by using columns with smaller inner diameters. Temperature effects do not appear to be a major source for concern in packed-column SFC.

INTRODUCTION

In supercritical fluid chromatography (SFC), retention is a strong function of the physical parameters of the system, *i.e.*, pressure and temperature[1]. Changes in retention can be most easily understood in terms of changes in the density of the mobile phase: the retention (capacity factor) will decrease regularly with increasing density. In most instances, the vapour pressure of the solute is not the main factor controlling retention in SFC and an increase in the pressure (at constant temperature) leads to an increased density and hence to a decrease in retention. An increase in temperature leads to a decrease in density (expansion) and hence to an increase in

0021-9673/87/$03.50

retention. Conversely, it can be shown that when the density is maintained constant, the retention is only marginally affected by temperature[1,2]. Although of secondary importance, the effect of the temperature is, however, not always negligible[3,4].

In the vicinity of the critical point, density is an extremely strong function of pressure[5]. For this reason, it is essential to control pressure rather than flow-rate in SFC. However, in order to achieve a flow of mobile phase through the column, it is a matter of principle that a pressure drop exists over the column. By approximation, Darcy's law can be assumed to be valid:

$$\Delta p = \eta L\, u/B^0 \tag{1}$$

where Δp is the pressure drop over the column (Pa), η the viscosity of the mobile phase (N s m^{-2}), L the column length (m), u the linear velocity of the mobile phase (m s^{-1}) and B^0 the specific permeability coefficient of the column (m^2).

For a packed column, the specific permeability coefficient is approximately

$$B^0 = d_p^2/1000 \tag{2}$$

where d_p is the particle diameter. For a typical packed SFC column[3] with $d_p = 10$ μm and $u = 0.5$ cm s^{-1} we find $B^0 \approx 10^{-13}$ m^2, and if we assume $\eta = 5 \cdot 10^{-5}$ N s m^{-2} for a typical supercritical fluid[6], we find for the pressure drop per unit column length $\Delta p/L \approx 2.5$ MPa m^{-1} or 25 bar m^{-1}. If we further assume the efficiency of such a column to be 40 000 plates per metre[3], then we find for the pressure drop per unit number of plates $\Delta p/(10^{-3}\ N) \approx 0.6$ bar. The pressure drop, both per unit length and per unit number of plates, will increase if the particle size is decreased.

For open (capillary) columns, we should use eqn. 3 instead of eqn. 2:

$$B^0 = d_c^2/32 \tag{3}$$

where d_c is the inner diameter of the column. For a typical capillary SFC column with $d_c = 50$ μm, eqn. 3 predicts $B^0 = 0.8 \cdot 10^{-10}$ m^2. If we assume a typical value for u of 2.4 cm s^{-1} (ref. 7) then we find $\Delta p/L = 15$ kPa m^{-1} (0.15 bar m^{-1}). If we further assume a typical efficiency for such a column[7,8] of 3000 plates m^{-1}, then $\Delta p/(10^{-3}\ N) = 0.05$ bar.

From this very simple calculation we conclude that the pressure drop per unit number of plates is about twelve times higher for packed-column SFC (10-μm particles) than for capillary SFC, but that in the latter instance the pressure drop over the column is still significant[9]. Moreover, as capillary columns are most commonly used to achieve high plate counts for the separation of complex samples, the columns are usually long (about 100 times longer than packed columns) and the actual pressure drop in typical capillary SFC will be of the same order as that in packed-column SFC. The main reason for this is not fundamental. It should be noted that the 3000 plates m^{-1} found in capillary SFC in practice is almost an order of magnitude lower than the theoretical value. Therefore, if more efficient stationary phases (in terms of mass transfer characteristics) can be developed for capillary SFC, then this could lead to a reduction in the column length and hence (eqn. 1) of the column pressure drop. Nevertheless, it is an important conclusion that the column pressure drop in

contemporary SFC is significant, when either packed or capillary columns are being used.

The above discussion provides some insight into the magnitude of the column pressure drop in SFC. However, it ought to be mentioned that the treatment is both simplified and incomplete. It is simplified because, when the pressure varies along the column, so does the density, and hence so do the linear velocity (u) and the viscosity (η). Therefore, the pressure gradient in the column is a function of the position along the column axis (z'):

$$\frac{dp}{dz'} = \frac{\eta(z')\, u(z')}{B^0} \tag{4}$$

Here, z' is a variable that represents the position along the column axis, in metres. A dimensionless parameter, $z = z'/L$, can be defined that varies between 0 and 1 (see Fig. 1a).

The treatment is also incomplete because of the strong variation of the viscosity of a supercritical fluid with density. Therefore, different values for η can be found under different experimental conditions (pressures and temperatures), even if the mobile phase is a single pure component.

It was the intention in this study to make more reliable estimates of the column pressure drop in packed-column SFC under various realistic experimental conditions, taking into account the variation of the pressure gradient along the column length according to eqn. 4.

Column temperature effects

In a previous study[9], we investigated the effects of the column pressure drop on the observed capacity factor. One of the remarkable findings was that the capacity factor decreased on decreasing the back-pressure (*i.e.*, the pressure at the column outlet), whilst keeping the inlet pressure constant. This observation is not in agreement with the simple statement above, that a decrease in pressure would lead to an increased capacity factor because of a decrease in the mobile phase density.

One of the possible explanations for this effect may be a lack of thermal equilibrium in the column. If an increase in the column pressure drop (resulting from a decrease in the back-pressure) were to result in a temperature drop of the mobile phase inside the column due to a (semi-)adiabatic expansion, then the (average) temperature in the column would decrease with an increase in the pressure drop, leading to an increase in the density and, therefore, to a decrease in the observed capacity factor.

In any case, the temperature inside the column may not always be assumed to be constant and equal to the temperature of the column wall. For high-performance liquid chromatography (HPLC), this was shown by Poppe *et al.*[10], who described the effects of viscous heat dissipation on the temperature of the mobile phase. In SFC the situation is more complex than it is in HPLC, because the compressibility of the mobile phase, which can be neglected with liquids, must be taken into account.

Therefore, in this work, we set out to model the physical transport processes of the mobile phase through the column in SFC with a view to predicting (1) the variation of the pressure along the length of the column, (2) the variation of the

temperature along the length of thhe column and (3) the radial temperature profile, *i.e.*, the variation of the temperature in a direction perpendicular to the column axis.

In a later paper[11] we shall report on the effects of variations in the column and particle dimensions on experimentally observed capacity factors. All calculations and experiments were performed with carbon dioxide as the mobile phase. Carbon dioxide is by far the most common eluent used in SFC and sufficient information on its physical properties is available to facilitate the model calculations described in this paper.

THEORETICAL MODEL

Fig. 1a shows a schematic representation of a column and illustrates the use of the dimensionless coordinates r (radial position in the column) and z (axial position). We have assumed a cylindrically symmetrical situation, *i.e.*, (p,T) conditions were assumed to be identical at all positions with given values of r and z. Pressure gradients in a radial direction were assumed to be absent, *i.e.*, p is a function $p(z)$ of z. $T(r,z)$ is a function describing the temperature, which we allowed to vary in both the radial and axial directions.

Fig. 1b illustrates the boundary conditions assumed in the calculations. The temperature of the mobile phase was assumed to be equal to the oven temperature (T_0) at the column inlet and along the column walls: $T(r,0) = T_0$ and $T(1,z) = T_0$. The column inlet pressure was fixed at $p(0) = p_{in}$. The mass flow of mobile phase equals φ_m at any value of z.

A heat balance for calculating temperature gradients in HPLC columns has been described by Poppe *et al.*[10]. Their treatment was based on three assumptions: (1) the mobile phase is incompressible; (2) effective heat transport properties of the mobile phase can be defined for the heterogeneous system inside the column (mobile phase, stationary phase and solid support); and (3) the mobile phase velocity is constant at any position in the column.

In SFC, a more complicated situation is encountered. The first assumption above is certainly invalid. An equation of state is required to describe the relationship between mobile phase density, pressure and temperature. The second assumption is no less valid for SFC than it is for HPLC. However, as the mobile phase density

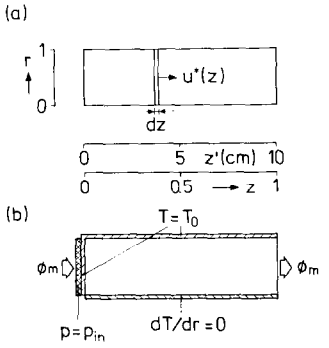

Fig. 1. Two schematic illustrations of a half column indicating (a) the coordinate system used in the calculations and (b) the boundary conditions applied. For explanation, see the text.

varies with the position in the column, so do the heat transport properties. The third assumption cannot be valid if the first is not. However, we did assume that radial variations in the linear velocity could be neglected ("plug flow").

Heat balance

The heat balance for the section dz of the column (see Fig. 1a) now reads

$$\frac{\partial T}{\partial t} = \frac{1}{L^2} \cdot \frac{\partial}{\partial z}\left(\frac{\lambda_{lon}}{\overline{\rho c}} \cdot \frac{\partial T}{\partial z}\right) + \frac{1}{R_c^2\, r} \cdot \frac{\partial}{\partial r}\left(\frac{\lambda_{rad} r}{\overline{\rho c}} \cdot \frac{\partial T}{\partial r}\right) - \frac{u\rho_m c_m}{L\overline{\rho c}} \cdot \frac{\partial T}{\partial z} - \frac{u}{L\overline{\rho c}} \cdot \frac{\partial p}{\partial z} - \frac{up}{Lv_m\overline{\rho c}} \cdot \frac{\partial v_m}{\partial z} \tag{5}$$

where the five terms on the right-hand side represent contributions from longitudinal heat conduction, radial heat conduction (including a contribution due to secondary flow in the radial direction), heat convection by flowing mobile phase, viscous heat dissipation and adiabatic expansion. The different terms will next be considered individually.

Heat conduction and convection

The heat conduction terms and the axial heat convection terms in eqn. 5 are similar to those encountered in HPLC[10]. However, the average heat capacity per unit volume of the heterogeneous system in the column ($\overline{\rho c}$) is a function of the position in the column. Neglecting the contribution of the (monomolecular) layer of stationary phase, we assumed

$$\overline{\rho c} = (1 - \varepsilon)\rho_{sil}c_{sil} + \rho_m c_m \varepsilon \tag{6}$$

where ε is the porosity of the column, ρ the density and c the specific (isochoric) heat capacity, and the subscripts sil and m denote the silica support and the mobile phase, respectively.

λ_{lon} is the longitudinal heat conductivity, which can be found from the heat conductivity of the silica support and that of the mobile phase in a manner analogous to eqn. 6. λ_{rad} includes a convective contribution due to so-called "eddy diffusion" (secondary flow around the particles)[10], so that

$$\lambda_{rad} = \lambda_{lon} + 0.03\, d_p u \rho_m c_m \tag{7}$$

Values of the density, the specific heat capacity and the heat conductivity of the silica support were taken to be 2 kg l^{-1}, 1.9 J g^{-1} K^{-1}, and 1.4 W m^{-1} K^{-1}, respectively[10]. The column porosity was assumed to be 0.58.

Viscous heat dissipation

The heat dissipation term in eqn. 5 bears a negative sign. This can easily be understood from the fact that dp/dz is a negative quantity. The pressure drop over

a small section of the column with length dz (see Fig. 1a) was calculated using eqn. 4. The viscosity η is a function of both pressure and temperature and, hence, varies with both r and z. A radially averaged viscosity (η^*) was calculated from

$$\eta^*(z) = 2\int_0^1 \eta(r,z)\, r\, \mathrm{d}r \tag{8}$$

using $p(z)$ and $T(r,z)$ to estimate $\eta(r,z)$.

Similarly, the (radially averaged) linear velocity $u(z)$ was obtained by first estimating the averaged density from

$$\rho^*(z) = 2\int_0^1 \rho(r,z)\, r\, \mathrm{d}r \tag{9}$$

and subsequently

$$u(z) = \frac{4\varphi_m}{\pi\varepsilon d_c^2\, \rho^*(z)} \tag{10}$$

where φ_m is the mass flow-rate of mobile phase through the column and d_c the inner diameter of the column.

Adiabatic expansion

Expansion of the mobile phase in the column may lead to a decrease in temperature. As the density (ρ_m) of the mobile phase decreases, its molar volume ($v_m = M/\rho_m$) increases, and therefore, dv_m/dz is a positive quantity. The viscous heat dissipation and adiabatic expansion terms can be seen to represent competitive effects. The former process causes an increase in the temperature of the effluent[10], whereas the latter process gives rise to a decrease. The process of adiabatic expansion can be formulated as

$$\mathrm{d}U = p\, \mathrm{d}V \tag{11}$$

where U is the energy content of the mobile phase and V its volume. In terms of the molar volume (v_m) and the number of moles (N_m), we find for the energy effect due to expansion

$$\frac{\mathrm{d}U}{\mathrm{d}t} = \frac{\mathrm{d}N_m}{\mathrm{d}t} \cdot p\, \mathrm{d}v_m \tag{12}$$

With

$$\mathrm{d}N_m/\mathrm{d}t = \varphi_m/M \tag{13}$$

and in the column segment with length $L\mathrm{d}z$

$$\mathrm{d}U = -\overline{\rho c}\, 2\pi R_c^2 \varepsilon L\, \mathrm{d}z\, \mathrm{d}T \tag{14}$$

we find

$$\frac{\partial T}{\partial t} = -\frac{\varphi_m p}{L\overline{\rho c}\, 2\pi R_c^2 \varepsilon M} \cdot \frac{\partial v_m}{\partial z} \tag{15}$$

Finally, with

$$\varphi_m = 2\pi\varepsilon R_c^2 u\, \rho_m \tag{16}$$

we find

$$\frac{\partial T}{\partial t} = -\frac{up}{L\overline{\rho c}\, v_m} \cdot \frac{\mathrm{d}v_m}{\mathrm{d}z} \tag{17}$$

or with $v_m = M/\rho_m$

$$\frac{\partial T}{\partial t} = \frac{up}{L\overline{\rho c}\, \rho_m} \cdot \frac{\mathrm{d}\rho_m}{\mathrm{d}z} \tag{17a}$$

The effect of the adiabatic expansion on the temperature in the column is seen to be proportional to the variation in the density of the mobile phase. This will be a function of two factors:

$$\frac{\mathrm{d}\rho_m}{\mathrm{d}z} = \frac{\mathrm{d}\rho_m}{\mathrm{d}p} \cdot \frac{\mathrm{d}p}{\mathrm{d}z} \tag{18}$$

The first factor follows from the equation of state and becomes larger the closer the critical point is approached. The second factor is the column pressure drop per unit length, which tends to increase with increasing flow-rate and with decreasing particle size (see eqns. 2 and 4). Therefore, the adiabatic expansion effect in packed column SFC may be expected to be larger (1) closer to the critical point, (2) at higher flow-rates and (3) with smaller particles.

PHYSICAL DATA

Equation of state

For the present calculations we used the analytical IUPAC equation of state, which closely describes pVT data for carbon dioxide, apart from the region very close to the critical point[5]. In this critical region a correction can be made, but for three reasons it was thought irrelevant in the present context to apply this refinement: (1) the complexity of the calculations would greatly increase; (2) other physical properties (heat capacity, viscosity) cannot be estimated with very high accuracy; and (3) the critical region is not very interesting from the point of view of practical SFC. The

last point is especially important. There are a number of cogent reasons for using SFC rather than critical fluid chromatography.

The analytical IUPAC equation of state reads

$$Z_m = \frac{pv_m}{RT} = \frac{pM}{\rho_m RT} = 1 + \rho_R \sum_{i=0}^{9} \sum_{j=0}^{6} b_{ij} \left(\frac{1}{T_R} - 1 \right)^j (\rho_R - 1)^i \qquad (19)$$

where Z_m is the compressibility coefficient of the mobile phase, R the gas constant, ρ_R the reduced density and b_{ij} are constants. The sum includes 70 terms, but 20 of the b_{ij} values are equal to zero. The b_{ij} values are listed in the Appendix (Table A.I).

The (critical) properties for carbon dioxide used in the calculations were T_c = 31.05°C, p_c = 72.865 atm (73.825 bar) and ρ_c = 0.466 g cm^{-3} (0.01059 mol cm^{-3}). The molar weight (M) of carbon dioxide is 44.009 g mol^{-1} and the gas constant (R) is 8.3143 J K^{-1} mol^{-1}.

Fig. 2 shows a pressure *versus* density plot, calculated from eqn. 19 by using the coefficients in Table A.I. (see Appendix) and the properties of carbon dioxide listed above.

Isochoric heat capacity

The isochoric heat capacity (c_v) can be found from a straightforward integration of the equation of state (eqn. 19) using

$$c_v = \int_0^{\rho} \frac{T}{\rho^2} \cdot \frac{\partial^2 p}{\partial T^2} \, d\rho + c_v^{id} \qquad (20)$$

where the superscript id denotes ideal gas conditions (zero pressure limit). c_v^{id} is related to c_p^{id} by

$$c_p^{id} - c_v^{id} = R \qquad (21)$$

Values for c_p^{id} were calculated using an empirical polynomial equation[5].

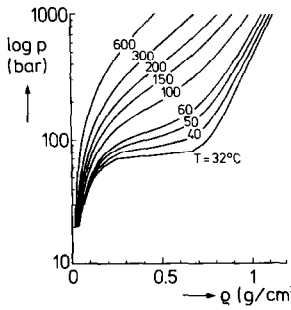

Fig. 2. Pressure *vs.* density curves calculated from the analytical IUPAC equation of state (eqn. 19) using the coefficients in Table A.I (Appendix).

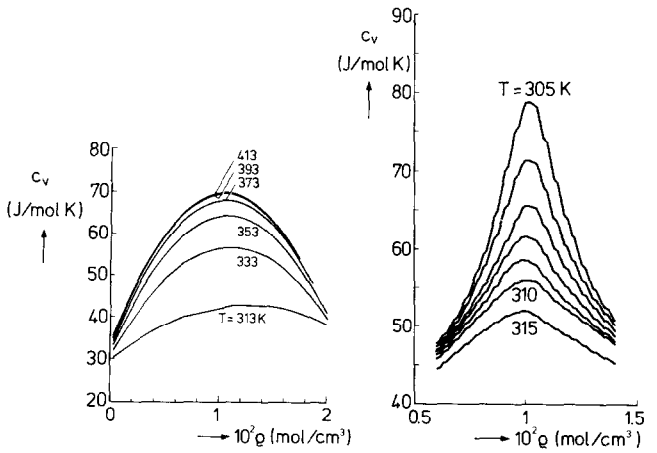

Fig. 3. (a) Values for the isochoric heat capacity, calculated using eqn. 22 with the coefficients in Tables A.I and A.II (Appendix) at temperatures of 40°C and above. (b) Interpolated values for c_v at temperatures between 40°C and the critical point using data from ref. 5, Table 7.

The resulting equation for c_v is

$$\frac{c_v}{T} = \left[\frac{1}{R_R^2}\sum_{i=0}^{9}\sum_{j=0}^{6} b_{ij}\cdot\frac{j(j-1)}{(i+1)}\left(\frac{1}{T_R}-1\right)^{j-2}(\rho_R-1)^{i+1}\right]_0^{\rho} + \sum_{n=0}^{7}\frac{\gamma_n}{T_R^n} - 1 \quad (22)$$

The values for ν_n in the c_p^{id} term are listed in the Appendix (Table A.II).

Fig. 3a shows the calculated isochoric heat capacity as a function of density at temperatures of 40°C and above. At temperatures close to the critical point, the above procedure was found to be inadequate. In these regions, we used the experimental data in ref. 5 (Table 7). Values for c_v at temperatures below 50°C were obtained by linear extrapolation. Fig. 3b shows some curves that were obtained in this way.

Thermal conductivity

For the thermal conductivity (λ^0) of carbon dioxide at low pressures we opted to use the simple Eucken equation:

$$\lambda^0 M/\eta = 4.47 + c_v \quad (23)$$

where M is the molecular weight, η the viscosity and c_v is in cal g^{-1} mol^{-1}. This equation has been claimed to yield "surprisingly good" results and to be "usually more accurate" than more complicated modified forms (see ref. 12, p. 495).

To estimate the thermal conductivity of carbon dioxide at higher pressures we used the equation given by Stiel and Thodos[13]:

$$(\lambda - \lambda^0)\xi Z_c^5 = A(e^{B\rho_R} - C) \quad (24)$$

where λ^0 can be found from eqn. 23, Z_c is the critical compressibility coefficient and ξ is a group defined as

$$\xi = T_c^{1/6} M^{-1/2} p_c^{-2/3} \tag{25}$$

The coefficients A, B and C have different values in different domains of the (reduced) density. The values are listed in the Appendix (Table A.III).

Fig. 4 shows the thermal conductivity calculated for carbon dioxide using eqns. 23–25 as a function of the reduced density at various temperatures.

Viscosity

The equation of Yoon and Thodos[14] for non-polar compounds was used to estimate the viscosity of carbon dioxide at low pressures:

$$\eta^0 \xi = 4.610 T_R^{0.618} - 2.04\, e^{-0.449 T_R} + 1.94\, e^{-4.058 T_R} + 0.1 \tag{26}$$

where ξ is given by eqn. 25.

For dense fluids ($0.1 < \rho_R < 3$) we used[15]

$$[(\eta - \eta^0)\xi + 1]^{0.25} = 1.023 + 0.23364\, \rho_R + 0.58533\, \rho_R^2 - 0.40758\, \rho_R^3 + 0.093324\, \rho_R^4 \tag{27}$$

Fig. 5 shows the calculated viscosity as a function of the (reduced) temperature for various values of the (reduced) pressure in the supercritical region.

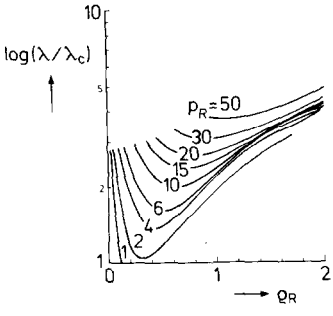

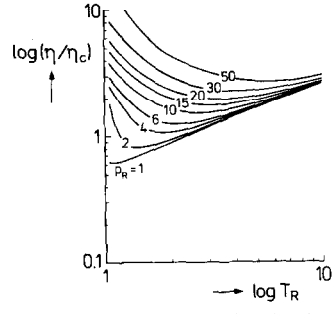

Fig. 4. Thermal conductivity of carbon dioxide as a function of the reduced density, calculated using eqns. 23–25 and the coefficients in Table A.III.

Fig. 5. Viscosity of supercritical carbon dioxide, calculated using eqn. 27, as a function of the reduced temperature for various values of the reduced pressure.

COMPUTATION METHODS

The differential equation for the heat balance (eqn. 5) cannot be solved analytically. Numerical computation methods have to be applied for the calculation of

the pressure and temperature profiles over the column. The procedure followed is summarized below.

(1) A grid is defined that covers the entire column, *i.e.*, $0 \leqslant r < 1$ and $0 \leqslant z < 1$. The grid is finest towards the ends and the walls of the column and coarse in the middle.

(2) An arbitrary pressure drop (*e.g.*, 5 bar) is assumed over the column, and the pressure gradient dp/dz is assumed to be constant. This yields the pressure $p(z)$ at each location in the column.

(3) The temperature at each location $[T(r,z)]$ is assumed to equal the oven temperature T_0.

(4) ρ_m, c_m, $\overline{\rho c}$, η, λ_{rad} and λ_{lon} are calculated as a function of r and z, using the calculated values of $p(z)$ and $T(r,z)$.

(5) dv_m/dz is calculated at each location from the density values computed at the locations $(r,z - dz)$ and $(r,z + dz)$.

(6) An optimal time interval, Δt, is determined, *i.e.*, Δt is taken as large as possible without reducing the accuracy of the calculations.

(7) At each location the differential equation is solved, keeping both the viscous heat dissipation and the adiabatic expansion terms constant (*i.e.*, independent of t). This process first takes place in one direction (*e.g.*, solving for dT/dz with r constant) and subsequently in the other (so-called split step method). This yields an estimate for ΔT at each location.

(8) The new temperature profile is calculated by adding the estimates for ΔT to the previous values. A radially averaged temperature, $T^*(z)$ is calculated from

$$T^*(z) = 2\int_0^1 T(r,z)\, r\, dr \tag{28}$$

(9) A new pressure profile is calculated, starting at the beginning of the column and using eqns. 4 and 10 and the viscosity and density calculated from eqns. 8 and 9, respectively.

(10) Steps 4–9 are repeated until all values for ΔT are smaller than a selected threshold value (stationary state; absolute accuracy better than 10^{-3} K, relative variation less than 10^{-10} s^{-1}).

When the above process is completed, pressure and temperature profiles, *i.e.*, $p(z)$ and $T(r,z)$, are obtained which satisfy the heat balance at every location in the column.

The calculations were performed on a VAX 8600 computer. All programs were written in FORTRAN 66. Use was made of subroutines from the NAG library (Numerical Algorithms Group, Oxford, U.K.).

RESULTS AND DISCUSSION

In Table I the results of a series of calculations under different sets of conditions are summarized. On the basis of these results, we may discuss the effects of pressure, temperature, (mass) flow-rate, particle size and column diameter on the pressure, density and temperature profiles in SFC columns.

TABLE I

CALCULATED PRESSURE, TEMPERATURE AND DENSITY VARIATIONS FOR COLUMNS OF LENGTH 10 cm

p_{in} (bar)	T_0 (°C)	φ_m (g min^{-1})	d_p (μm)	I.D. (mm)	Δp (bar)	ρ_{in} (g ml^{-1})	ρ^* ($z = 1$) (g ml^{-1})	$10^3\Delta T^*$ (°C)	$10^3\Delta T$ ($r = 0$) (°C)	t_0 (s)
80	35	0.1	8	4.6	0.21	0.449	0.434	− 1	− 2	255.4
80	35	1	8	4.6	2.10	0.449	0.345	−79	−157	22.8
80	35	0.189	8	2	2.11	0.449	0.342	−14	− 38	22.5
80	40	1	8	4.6	2.38	0.282	0.257	−34	− 68	15.6
80	50	1	10	4.6	1.76	0.220	0.211	−15	− 30	12.5
80	50	1	8	4.6	2.83	0.220	0.205	−24	− 48	12.3
80	50	1	5	4.6	5.37	0.220	0.184	−60	−119	11.7
80	50	1	4	4.6	11.99	0.220	0.165	−95	−190	11.1
80	100	1	8	4.6	4.28	0.142	0.132	−15	− 30	7.9
90	35	0.5	8	4.6	1.08	0.663	0.655	− 0	− 0	76.2
90	35	1	8	4.6	2.16	0.663	0.646	− 1	− 2	37.9
90	35	0.189	8	2	2.16	0.663	0.646	− 0	− 0	37.9
90	35	0.047	8	1	2.16	0.663	0.646	− 0	− 0	37.9
100	35	1	8	4.6	2.22	0.712	0.704	+ 2	+ 5	40.9
150	35	1	8	4.6	2.37	0.813	0.810	+ 4	+ 7	46.9
150	35	3	8	4.6	7.08	0.813	0.804	+33	+ 66	15.6
150	40	1	8	4.6	2.32	0.779	0.775	+ 4	+ 7	44.9
150	40	3	8	4.6	6.93	0.779	0.767	+31	+ 62	14.9
150	50	1	8	4.6	2.33	0.700	0.694	+ 3	+ 5	40.3
150	100	1	8	4.6	2.43	0.333	0.326	− 6	− 11	19.1
150	100	3	8	4.6	7.37	0.333	0.310	−55	−109	6.2

The five variables are listed as the first five entries in Table I. Δp is the calculated pressure drop over the column. ρ_{in} is the mobile phase density at the column inlet; $\rho^*(z = 1)$ is the radially averaged density of the mobile phase at the column exit. ΔT^* is the difference between the radially averaged temperature at the end of the column ($z = 1$) and the oven temperature [*i.e.* $\Delta T^* = T^*(z = 1) - T_0$]; $\Delta T(r = 0)$ is the temperature effect in the middle of the column [*i.e.*, $\Delta T(r = 0) = T(z = 1; r = 0) - T_0$]. Finally, t_0 is the hold-up time (elution time of an unretained solute) of the column, which can be calculated once the density profile over the column is known.

Calculations were performed successfully, assuming a wide variety of experimental conditions. However, the number of iterations and the computation time required to reach a satisfactory solution for the heat balance equation was higher in those instances where large density variations occur. Generally, the calculations became more difficult (1) the lower the column inlet pressure, (2) the lower the temperature, (3) the higher the flow-rate and (4) the smaller the particle size.

As all calculations were performed in the supercritical region, lowering the pressure or temperature implied approaching the critical point more closely. It is worth noting that the computation process accurately reflects our practical experience. At operating conditions very close to the critical point it is difficult to achieve

stable, reproducible conditions in practice, and this is certainly even truer at higher flow-rates and/or with smaller particle sizes.

Under one set of conditions, we were not able to obtain a satisfactory solution for the heat balance, *viz.*, at an inlet pressure of 80 bar, a temperature of 35°C and a mass flow-rate of 3 g min^{-1} (for a 4.6-mm I.D. column packed with 8-μm particles). During the calculation process, conditions were inevitably obtained that were critical rather than supercritical. However, this particular set of conditions cannot be used in practice.

The present model is not strictly limited to the supercritical region. For example, at an inlet pressure of 80 bar, a pressure drop of about 12 bar was observed with a particle size of 4 μm, causing the outlet pressure to be well below the critical value. However, at a temperature of 50°C the critical point is not approached too closely.

Pressure and density effects

Fig. 6 shows some calculated profiles of the pressure along the length of the column at inlet pressures of 80 and 150 bar and at various temperatures. Linear profiles are obtained at an inlet pressure of 150 bar. More remarkably, at an inlet pressure of 80 bar the curves are still virtually linear, even though a considerable expansion takes place in the column, as indicated by the densities listed in Table I. The explanation for the linear pressure profiles is that the viscosity is (very) roughly proportional to the density. When the mobile phase expands in the column, the linear velocity will be inversely proportional to the density. Therefore (eqn. 4), the rate of pressure drop is roughly constant along the length of the column. Only when the changes in the mobile phase density become very large can a distinct curvature of the pressure profiles be observed. This is illustrated in Fig. 7, where the effect of the particle size on the pressure profile is shown. Convex curves are obtained if 5- or 4-μm particles are used. The curvature will be more pronounced if the temperature is closer to that of the critical point.

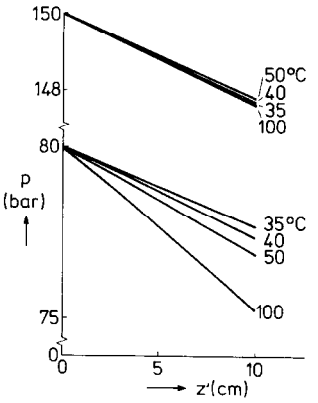

Fig. 6. Pressure profiles for packed columns in SFC for various (inlet) pressures and oven temperatures. Mobile phase, carbon dioxide; mass flow-rate, 1 g min^{-1}; column I.D., 4.6 mm; particle size, 8 μm.

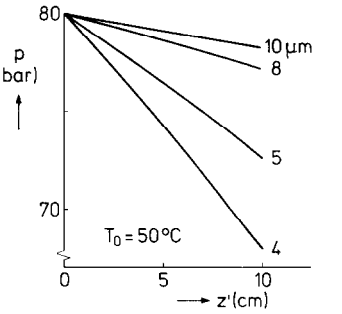

Fig. 7. Pressure profiles for packed columns in SFC for various particle sizes. Mobile phase, carbon dioxide; inlet pressure, 80 bar; oven temperature, 50°C; mass flow-rate, 1 g min^{-1}; column I.D., 4.6 mm.

Fig. 8 shows some examples of density profiles obtained at various inlet pressures and a temperature just above the critical point. It is seen that the variations in density are small as soon as the pressure is well above the critical value of 73.8 bar. At higher pressures, the supercritical fluid behaves in nearly the same way as an incompressible liquid. This is supported by other data in Table I, which show the influence of the flow-rate. At a pressure of 90 bar, the pressure drop is seen to be proportional to the flow-rate and the hold-up time is almost exactly inversely proportional to the flow-rate. At 150 bar, this is even truer. Hence, under conditions away from the critical point, SFC resembles HPLC, but the viscosity of the eluent and hence the pressure drop are low.

Fig. 9 illustrates that the variations in the mobile phase density increase if the particle size is decreased, as expected. A smooth, almost linear decrease in mobile phase density is obtained.

Temperature effects

In Table I both positive and negative values for the temperature effect are observed. A negative temperature effect indicates that the contribution of adiabatic expansion dominates, whereas a positive temperature effect is caused by viscous heat dissipation. At high densities (*e.g.*, at p_{in} = 150 bar and T_0 between 35 and 50°C) the fluid behaves like a liquid, and the temperature effect is positive. However, because of the relatively low viscosity of supercritical fluids, the rise in temperature is always small compared with that in HPLC[10]. The temperature effect rapidly increases as the flow-rate is increased.

When the density is lower [due either to a lower column inlet pressure (*e.g.*, 80 bar) or to a higher temperature (*e.g.*, 100°C)], the adiabatic expansion term in eqn. 5 becomes larger than the contribution from viscous heat dissipation. However, the observed temperature effects are never very large. Typically, variations in the radially averaged temperature are within *ca.* 0.1°C. The variations in temperature at the centre of the column are twice as large, indicating a parabolic radial temperature profile. Such variations in temperature do have a significant effect on the density in the vicinity of the critical point. However, at low flow-rates the temperature effects be-

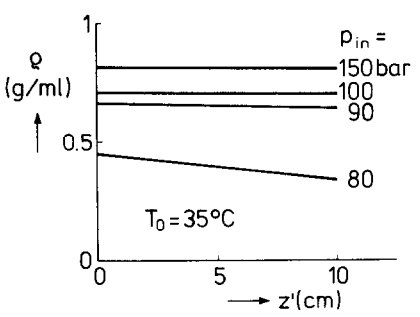

Fig. 8. Density profiles for packed columns in SFC for various (inlet) pressures. Mobile phase, carbon dioxide; oven temperature, 35°C; mass flow-rate, 1 g min^{-1}; column I.D., 4.6 mm; particle size, 8 μm.

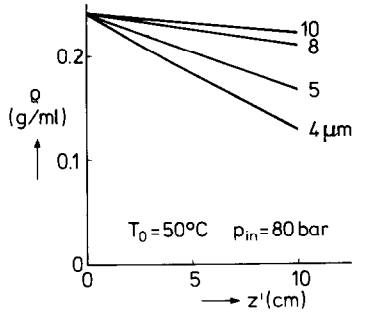

Fig. 9. Density profiles for packed columns in SFC for various particle sizes. Mobile phase, carbon dioxide; inlet pressure, 80 bar; oven temperature, 50°C; mass flow-rate, 1 g min^{-1}; column I.D., 4.6 mm.

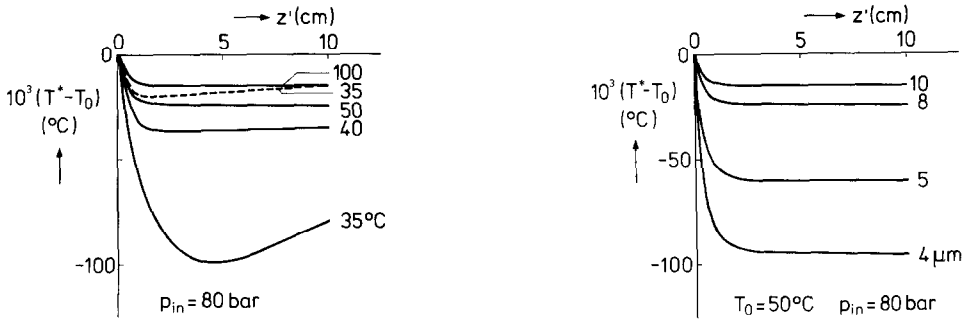

Fig. 10. Temperature profiles for packed columns in SFC at various oven temperatures. Mobile phase, carbon dioxide; inlet pressure, 80 bar; mass flow-rate, 1 g min^{-1}; column I.D., 4.6 mm (solid lines) or 2 mm (dashed line); particle size, 8 μm.

Fig. 11. Temperature profiles for columns in SFC packed with various particle sizes. Mobile phase, carbon dioxide; inlet pressure, 80 bar; oven temperature, 50°C; mass flow-rate, 1 g min^{-1}; column I.D., 4.6 mm.

come minimal, so that they cannot be held responsible for anomalous retention behaviour under these conditions, as we have suggested previously[9]. This conclusion is correct if a similar retention behaviour is obtained when columns of smaller diameters are used. Such experiments are currently being performed in our laboratory[11].

Fig. 10 shows the temperature profiles in the axial direction at various temperatures, an inlet pressure of 80 bar and a mass flow-rate of 1 g min^{-1}. It is seen that the temperature effects are largest in the direct vicinity of the critical point (T_0 = 35°C). At this lowest temperature, the temperature is seen to be passing through a minimum, roughly in the middle of the 10-cm long column. Such a minimum was frequently calculated at column temperatures close to the critical value.

The dashed line in Fig. 10 represents a column with a reduced inner diameter (2 mm). The mass flow-rate for this column has been reduced in such a way that the mass flux (flow per unit area) is kept constant. It is seen that the temperature effect can be greatly reduced in this way. At an inlet pressure of 80 bar, a small difference can be observed in the density at the column outlet between columns of 4.6 and 2 mm I.D. (see Table I). Also, there is a difference in the calculated value of t_0. Similar calculations at an inlet pressure of 90 bar, only slightly further removed from the critical point, indicate that this is no longer the case (see Table I).

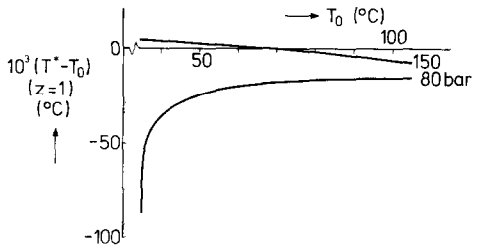

Fig. 12. Temperature effects for packed columns in SFC at various oven temperatures and two different inlet pressures. Mobile phase, carbon dioxide; mass flow-rate, 1 g min^{-1}; column I.D., 4.6 mm.

Fig. 11 shows the observed temperature profiles at 80 bar and 50°C for columns packed with particles of various sizes. The temperature effects are seen to increase considerably when the particle size is reduced. However, considering that these data are obtained at pressures close to the critical value, the absolute magnitude of the temperature effect is still not very large.

Fig. 12 summarizes some of the calculated temperature effects at various temperatures and column inlet pressures of 150 and 80 bar. At 150 bar, the temperature effect is always very small. It is slightly positive at low temperatures (high densities) and slightly negative at high temperatures (low densities). At an inlet pressure of 80 bar the temperature effect is always negative. It is seen to increase very rapidly if the temperature approaches the critical value. However, temperatures very close to the critical point are not attractive for practical operating conditions, so that these "large" temperature effects will not usually be encountered.

As a conclusion, we may say that the temperature effect is unlikely to form a major obstacle for packed-column SFC. If, under conditions close to the critical point, using high flow-rates and/or very small particles, the temperature effect should become significant, then it may be effectively minimized by reducing the diameter of the column.

Hold-up times

Fig. 13 illustrates the variation of the (calculated) hold-up time (t_0) with the column temperature at two different pressures. At a constant mass flow-rate the hold-up time is determined by the density of the mobile phase. If the density is constant throughout the column, as is roughly the case at 150 bar, then t_0 may be estimated from the density calculated for the conditions at the column inlet. When large variations in the density occur along the column length (*e.g.*, at 80 bar), then a more sophisticated calculation procedure, such as that described in this paper, is required for estimating the value of t_0.

CONCLUSIONS

The procedure described here allows the calculation of pressure, density and temperature profiles for SFC with packed columns and carbon dioxide as the mobile phase. The (mass) flow-rate, the particle size and the column diameter are additional

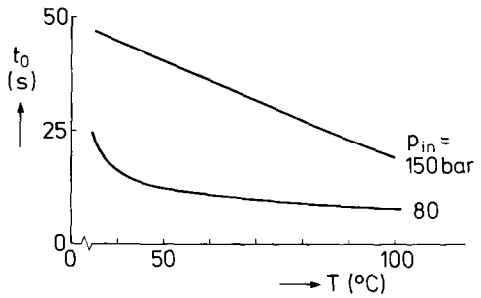

Fig. 13. Calculated hold-up times for packed columns in SFC at various oven temperatures and two different inlet pressures. Mobile phase, carbon dioxide; mass flow-rate, 1 g min^{-1}; column I.D., 4.6 mm.

variables that can be changed in the program. These calculations provide an insight into the behaviour of SFC columns. The results can be summarized as follows:

(1) Pressure profiles along packed columns for SFC are approximately linear, because an increase in the linear velocity is compensated by a decrease in the viscosity.

(2) Density profiles are linear or slightly convex. If the density of the mobile phase is high, it changes little over the length of the column. At lower densities the variations are greater.

(3) Depending on the operating conditions, temperature effects in SFC may be negative (cooling due to adiabatic expansion) or positive (heating due to viscous heat dissipation). Temperature effects are larger (i) closer to the critical point, (ii) at higher flow-rates and (iii) with smaller particles. There is a parabolic radial temperature profile over the column.

(4) Temperature effects are unlikely to be a major problem in packed-column SFC. The effects may be reduced by using columns with a smaller inner diameter.

We experienced two limitations of the present model. First, it only enables us to calculate the stationary state. Sometimes, especially in the vicinity of the critical point, it takes a long time to achieve a stationary state. The model does not reveal anything about this process. Second, adsorption of mobile phase molecules at the surface of the stationary phase is not taken into account. We feel that this second factor may have a significant effect on the retention process in SFC. However, at present, no data are available that would allow us to introduce a separate carbon dioxide adsorption term in eqn. 5.

Despite the limitations described above, we feel that this study has clarified some of the physical processes that occur in packed SFC columns and that the results may be of help in designing and operating SFC instruments.

LIST OF SYMBOLS

Listed here are the symbols that occur in the text, their meanings and (in parentheses) the units in which they are expressed, unless indicated otherwise in the text.

A	coefficient in the Stiel and Thodos equation (eqn. 24)
b_{ij}	coefficients in the equation of state (eqn. 19)
B	coefficient in the Stiel and Thodos equation (eqn. 24)
B^0	specific permeability coefficient (m^2)
c	specific isochoric heat capacity ($J\ g^{-1}\ K^{-1}$)
C	coefficient in the Stiel and Thodos equation (eqn. 24)
d_c	column diameter (m)
d_p	particle size (m)
L	column length (m)
M	molecular weight ($g\ mol^{-1}$)
N	number of theoretical plates
N_m	number of moles of mobile phase
p	pressure (Pa)
p_{in}	column inlet pressure (Pa)
r	dimensionless coordinate perpendicular to the column axis
R_c	column radius

R	gas constant (J mol^{-1} K^{-1})
t	time (s)
T	absolute temperature (K)
T_0	oven temperature (K)
u	mobile phase linear velocity (m s^{-1})
U	internal energy (J)
v	molar volume (m^3 mol^{-1})
V	volume (m^3)
z	dimensionless coordinate along the column axis
z'	coordinate along the column axis (m)
Z	compressibility coefficient

Subscripts

c	critical, column
lon	longitudinal
m	mobile phase
p	isobaric
rad	radial
R	reduced
sil	silica support
v	isochoric

Superscripts

0	zero pressure limit
id	ideal gas
*	radial average

Greek symbols

γ_n	coefficients in heat capacity equation (eqn. 22)
ε	column porosity
η	viscosity (N s m^{-2})
λ	heat conductivity (W m^{-1} K^{-1})
ξ	dimensionless group defined by eqn. 25 ($K^{1/6}$ $atm^{-2/3}$)
ρ	density (kg m^{-3})
$\overline{\rho c}$	average heat capacity per unit volume of the column (J m^{-3} K^{-1})
φ_m	mobile phase mass flow-rate (g s^{-1})

ACKNOWLEDGEMENT

For solving the heat balance equation, use was made of the TEDDY program package of the Philips Information Systems and Automation (ISA) Corporate CAD centre.

APPENDIX

Coefficients for equations describing the physical properties of carbon dioxide

Equation of state. The coefficients b_{ij} for the analytical equation of state are listed in Table A.I.

TABLE A.I.

COEFFICIENTS FOR THE IUPAC ANALYTICAL EQUATION OF STATE FOR CARBON DIOXIDE (EQN. 19)

Values for b_{ij} were taken from ref. 5.

i	$j = 0$	$j = 1$	$j = 2$	$j = 3$
0	− 0.725854437	−1.68332974	0.259587221	0.376945574
1	0.447869183	1.26050691	5.96957049	15.4645885
2	− 0.172011999	−1.83458178	− 4.61487677	− 3.82121926
3	0.00446304911	−1.76300541	−11.1436705	−27.8215446
4	0.255491571	2.37414246	7.50925141	6.61133318
5	0.0594667298	1.16974683	7.43706410	15.0646731
6	− 0.147960010	−1.69233071	− 4.68219937	− 3.13517448
7	0.0136710441	−0.100492330	− 1.63653806	− 1.87082988
8	0.0392284575	0.441503812	0.886741970	0
9	− 0.0119872097	−0.0846051949	0.0464564370	0

	$j = 4$	$j = 5$	$j = 6$
0	− 0.670755370	−0.871456126	− 0.149156928
1	19.4449475	8.64880497	0
2	3.60171349	4.92265552	0
3	−27.1685720	−6.42177872	0
4	− 2.42663210	−2.57944032	0
5	9.57496845	0	0
6	0	0	0
7	0	0	0
8	0	0	0
9	0	0	0

Isochoric heat capacity. Table A.II gives the values for γ_n for use in eqn. 20 to calculate the isochoric heat capacity of carbon dioxide.

TABLE A.II

COEFFICIENTS FOR THE EQUATION FOR THE ISOCHORIC HEAT CAPACITY OF CARBON DIOXIDE (EQN. 20)

Values for γ_n were taken from ref. 5.

n	γ_n
0	7.69441246
1	− 0.249610766
2	−25.4000397
3	65.1102201
4	−82.0863624
5	57.4148450
6	−21.2184243
7	3.23362153

Thermal conductivity. Table A.III lists the coefficients for the Stiel and Thodos equation for the thermal conductivity (eqn. 24) for three different ranges of density.

TABLE A.III

COEFFICIENTS FOR THE CALCULATION OF THE THERMAL CONDUCTIVITY OF CARBON DIOXIDE (EQN. 24) IN VARIOUS DOMAINS OF THE REDUCED DENSITY[13]

Density domain	10^8 *A*	*B*	*C*
$\rho_R < 0.5$	14.0	0.67	1
$0.5 \leqslant \rho_R < 2$	13.1	0.67	1.069
$2 \leqslant \rho_R < 2.8$	2.976	1.155	2.016

REFERENCES

1 P. J. Schoenmakers, *J. Chromatogr.*, 315 (1984) 1.
2 U. van Wasen, I. Swaid and G. M. Schneider, *Angew. Chem.*, 92 (1980) 58.
3 D. R. Gere, R. Board and D. McManigill, *Anal. Chem.*, 54 (1982) 736.
4 C. R. Yonker and R. D. Smith, *J. Chromatogr.*, 351 (1986) 211.
5 IUPAC, *International Thermodynamic Tables of the Fluid State — Carbon Dioxide*, Pergamon Press, Oxford, 1973.
6 P. J. Schoenmakers and F. C. C. J. G. Verhoeven, *Trends Anal. Chem.*, 6 (1) (1987) 10.
7 W. P. Jackson, B. E. Richter, J. C. Fjeldsted, R. C. Kong and M. L. Lee, in S. Ahuja (Editor), *Ultrahigh Resolution Chromatography*, ACS Symposium Series, Vol. 250, American Chemical Society, Washington, DC, 1984, pp. 121–133.
8 S. M. Fields, R. C. Kong, M. L. Lee and P. A. Peaden, *J. High Resolut. Chromatogr. Chromatogr. Commun.*, 7 (1984) 423.
9 P. J. Schoenmakers and F. C. C. J. G. Verhoeven, *J. Chromatogr.*, 352 (1986) 315.
10 H. Poppe, J. C. Kraak, J. F. K. Huber and J. H. M. van den Berg, *Chromatographia*, 14 (1981) 515.
11 P. J. Schoenmakers and L. G. M. Uunk, to be presented at the *11th International Symposium on Column Liquid Chromatography, Amsterdam, 28 June–3 July, 1987.*
12 R. J. Reid, J. M. Prausnitz and T. K. Sherwood, *The Properties of Gases and Liquids*, McGraw-Hill, New York, 3rd ed., 1977.
13 L. I. Stiel and G. Thodos, *AIChE. J.*, 10 (1964) 26.
14 P. Yoon and G. Thodos, *AIChE J.*, 16 (1970) 300.
15 J. A. Jossi, L. I. Stiel and G. Thodos, *AIChE J.*, 8 (1962) 59.